Landslide Susceptibility Mapping along NH-7 in the Himalayas using Frequency Ratio Method

Khyati Gupta* and Tariq Siddique

Department of Geology, Aligarh Muslim University, Aligarh - 202001, Uttar Pradesh, India

* Corresponding author

doi: https://doi.org/10.21467/proceedings.179.17

ABSTRACT

The main aim of this study is the evaluation of landslide susceptibility along NH-7 from Karnaprayag to Joshimath, Uttarakhand by employing the frequency ratio method in the GIS environment. For the analysis of landslide vulnerability, 83 landslide points were identified. Sixteen layers of landslide causative elements were prepared, including slope angle, soil, slope aspect, seismicity, elevation, proximity to road, proximity to faults, lithology, proximity to stream, topographic wetness index (TWI), rainfall, normalized difference vegetation index (NDVI), plan curvature, land use and land cover (LULC), stream power index (SPI) and profile curvature. An inventory map of landslide events was generated. Further, for the assessment of landslide susceptibility, the evaluation of frequency ratio for each conditioning factor was assessed. The model was validated using ROC(AUC) curves. The value for success rate curve (SRC) is 85.5%, while for the prediction rate curve (PRC) is 84.1%. The model is in good agreement with the distribution characteristics of past landslides in the study area. Land-use planners and decision-makers may utilize the results to manage and mitigate potential landslides, safeguarding the ecology and preserving society.

Keywords: Landslides susceptibility mapping. Landslide Conditioning Factors. Frequency Ratio Method. ROC-AUC.

1. Introduction

In India, the Garhwal Himalayas are comprised of steep mountain ranges resulting from orogenesis. Landslides are frequently observed in the higher sections of the Alaknanda Valley in the Garhwal Himalayas, particularly from Chamoli to Pipalkoti and above to Badrinath. The key factors causing slope instability are steep slope angle, deforestation, excessive precipitation and construction of new roads [1]–[3]. The magnitude to which topography can be affected by slope movements or the where landslides are most likely to occur is known as landslide susceptibility [4]. Generally, the methods of modeling landslide susceptibility are categorised into two broad categories as qualitative and quantitative [5], [6]. Quantitative methods are mostly favoured over qualitative methods due to the higher accuracy of the results. The current work concentrates on landslide susceptibility mapping along NH-7 from Karnaprayag to Joshimath, utilizing the frequency ratio method. The interpretation of the frequency ratio model was assessed using the success rate curve and prediction rate curve.

2. Study area

The study is conducted on 80 km stretch along the national highway (NH-7) from Karnaprayag to Joshimath (Figure 1). The area lies in Chamoli district, extending between 30°16´44´´N to 30°33´10´´N latitudes and 79°13´12´´E to 79°32´48´´ E longitudes. The area is approachable through road link and is 168 km from Rishikesh. Geologically, the area belongs to the Lesser and the Higher Himalayas and

© 2025 Copyright held by the author(s). Published by AIJR Publisher in "Proceedings of the Second International Conference in Civil Engineering for a Sustainable Planet: ICCESP 2024". Organized on 6-8 December 2024, by Habilete Learning Solutions, Kollam, Kerala, India in collaboration with. Marian Engineering College, Trivandrum, Kerala; American Society of Civil Engineers (ASCE); and ASCE India Section southern Region.

Proceedings DOI: 10.21467/proceedings.179; Series: AIJR Proceedings; ISSN: 2582-3922; ISBN: 978-81-984081-7-4

is heavily dissected by numerous faults and thrusts, which makes it a seismically active terrain. The rocks near Helang town are intensely sheared due to Main Central Thrust (MCT) [7]–[10]. The major rock type found in the region is metasedimentary type, including dolomites or limestones, slates, quartzites, phyllites, schists and gneisses [11], [12].

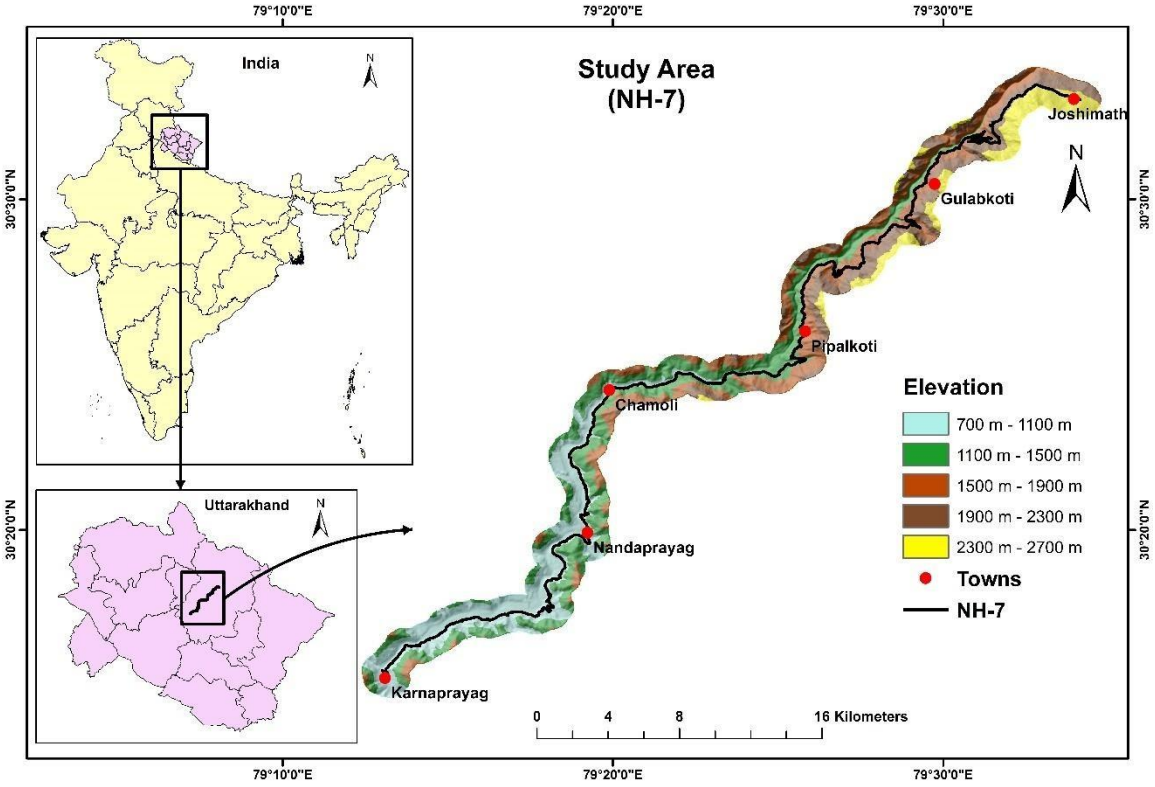

Figure 1. Study area map

3. Methodology

The process of landslide susceptibility mapping involves five steps [13] as follows: (a) gathering data and setting up a spatial database; (b) assessing the association between landslide inventories and conditional factors in order to assess landslide susceptibility; (c) figuring out frequency ratio of conditional factors; (d) result validation; (e) apprehension of the results. Sixteen landslide conditioning factors were selected for the preparation of landslide susceptibility map of the study area. These were, namely- slope aspect, proximity to fault, proximity to road, elevation, proximity to stream, lithology, normalized difference vegetation index (NDVI), plan curvature, land-use/landcover (LULC), profile curvature, rainfall, seismicity, stream power index (SPI), slope angle, soil and topographic wetness index (TWI). ArcGIS software has been used to prepare thematic layers (Figure 2) of the conditioning factors for the 1 km buffer zone on either side of the road (NH7). All the layers were projected in Universal Transverse Mercator (UTM-44N) projection system.

Proceedings DOI: 10.21467/proceedings.179
ISBN: 978-81-984081-7-4

Series: AIJR Proceedings
ISSN: 2582-3922

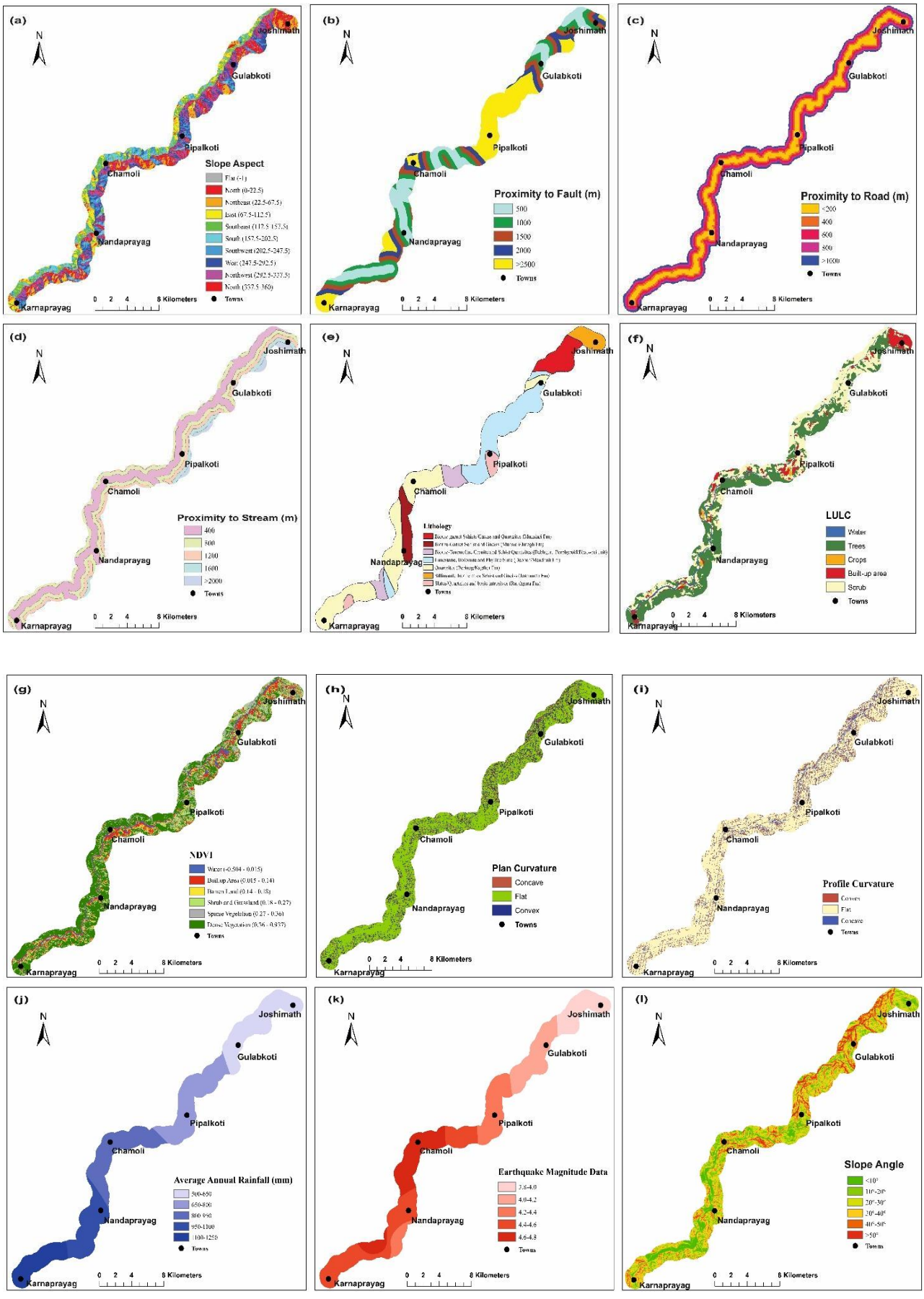

Proceedings DOI: 10.21467/proceedings.179
ISBN: 978-81-984081-7-4

Series: AIJR Proceedings
ISSN: 2582-3922

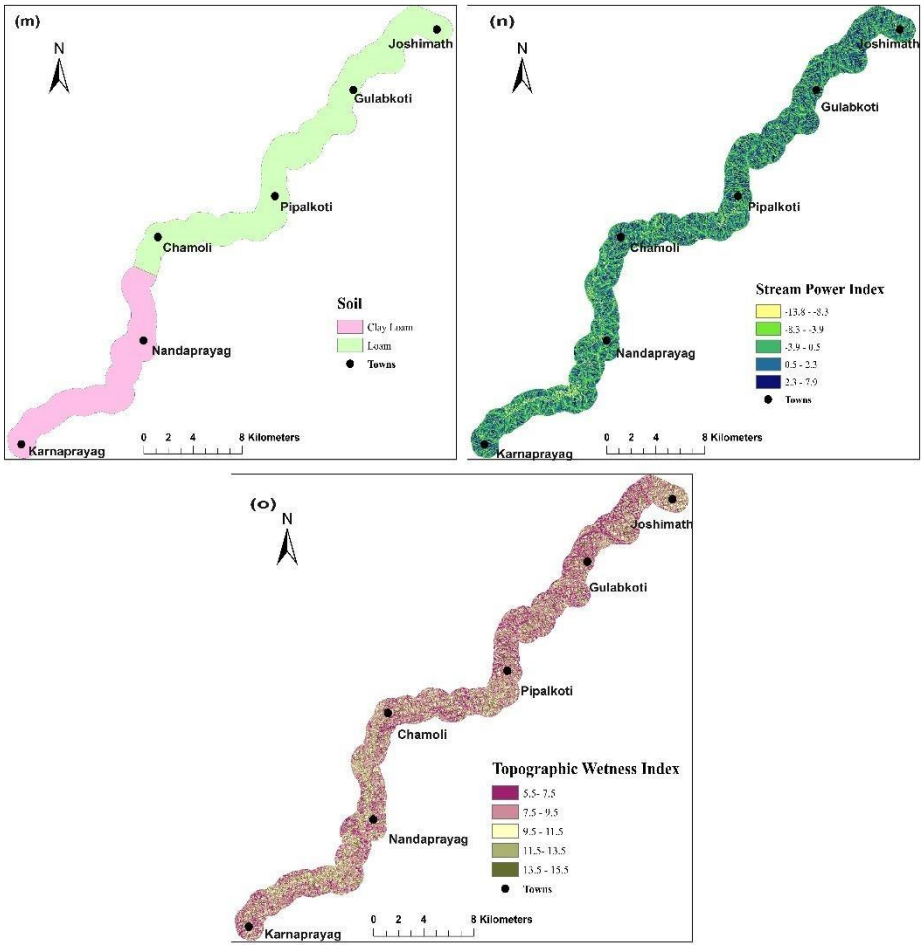

Figure 2. Thematic layers of all landslide conditioning factors

Digital elevation model (DEM) of 30 m resolution of the study was prepared from SRTM (Shuttle Radar Topography Mission) derived from USGS Earth Explorer [14]. Proximity to road/stream/fault, elevation, plan curvature, slope angle, profile curvature, slope aspect, SPI and TWI maps were prepared from the DEM image. LULC map was prepared from ESRI Sentinal-2 10 m land-use/landcover map [15] and USGS Sentinal-2 data [16] was used to construct NDVI map. University of East Anglia Climatic Research Unit (CRU TS4.0) [17] has 0.5° gridded data which was used to obtain rainfall data and to generate a rainfall map. To generate the soil map of the study area, data from FAO/UNECSO digital soil map of the world at a scale of 1:5000000 was utilized. The landslide inventory map (Figure 3) of the study area was prepared from Bhukosh, Geological Survey of India portal [18]. For this study, 83 landslide points in the study area have been identified and verified from Google Earth.

Proceedings DOI: 10.21467/proceedings.179
ISBN: 978-81-984081-7-4

Series: AIJR Proceedings
ISSN: 2582-3922

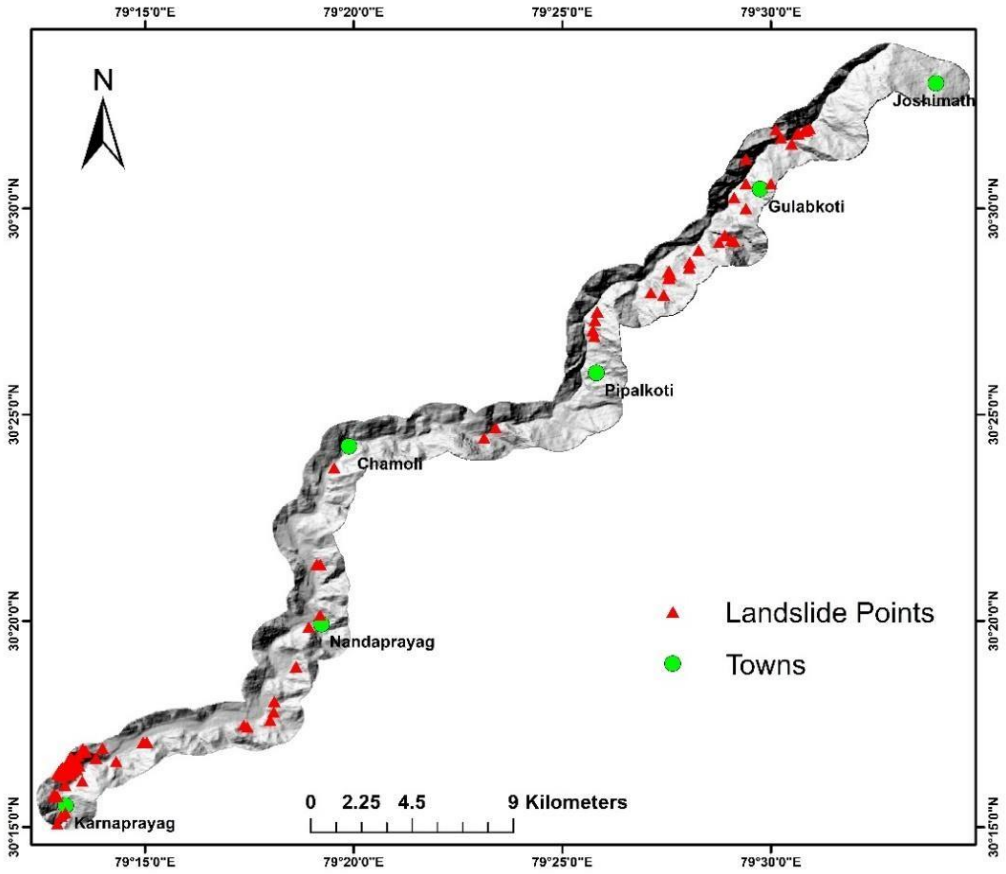

Figure 3. Landslide inventory map

The frequency ratio (FR) model has been used to assess the landslide susceptibility of the study area. FR is frequently employed to comprehend the potential association between current landslide incidents and causative geo-factors. FR is calculated from the frequency ratio values, which represent the ratio of the likelihood of existence and non-existence of landslides for each landslide conditioning factor class. It is calculated by using the following equation [13], [19]–[22]:

$$FR = \frac{\frac{N_i^{pix}}{N}}{\frac{N_i^{Lpix}}{N^L}}$$

N_i^{pix} = number of pixels per conditioning factor class

N = total number of pixels in the study area

N_i^{Lpix} = number of landslide pixels per conditioning factor class

N^L = total number of landslide pixels in the study area

The FR value of >1 indicates a positive correlation and high landslide susceptibility. In contrast, a negative correlation and low landslide susceptibility are depicted by a value < 1. The FR values of each class of all landslide conditioning factors were calculated using Microsoft Excel.

Proceedings DOI: 10.21467/proceedings.179
ISBN: 978-81-984081-7-4

Series: AIJR Proceedings
ISSN: 2582-3922

4. Results and Discussion

After calculating the FR values, prediction ratio (PR) for each conditioning factor was calculated (Table 1). PR values were then used to build the final landslide susceptibility map in Arc GIS software by using following equation [13].

$$LSM = \sum Each\ conditioning\ factor\ \times PR\ value$$

Based on the results (Figure 4), 87% of total landslides occur in the high and very high zones of the susceptibility map of the research area (Table 2).

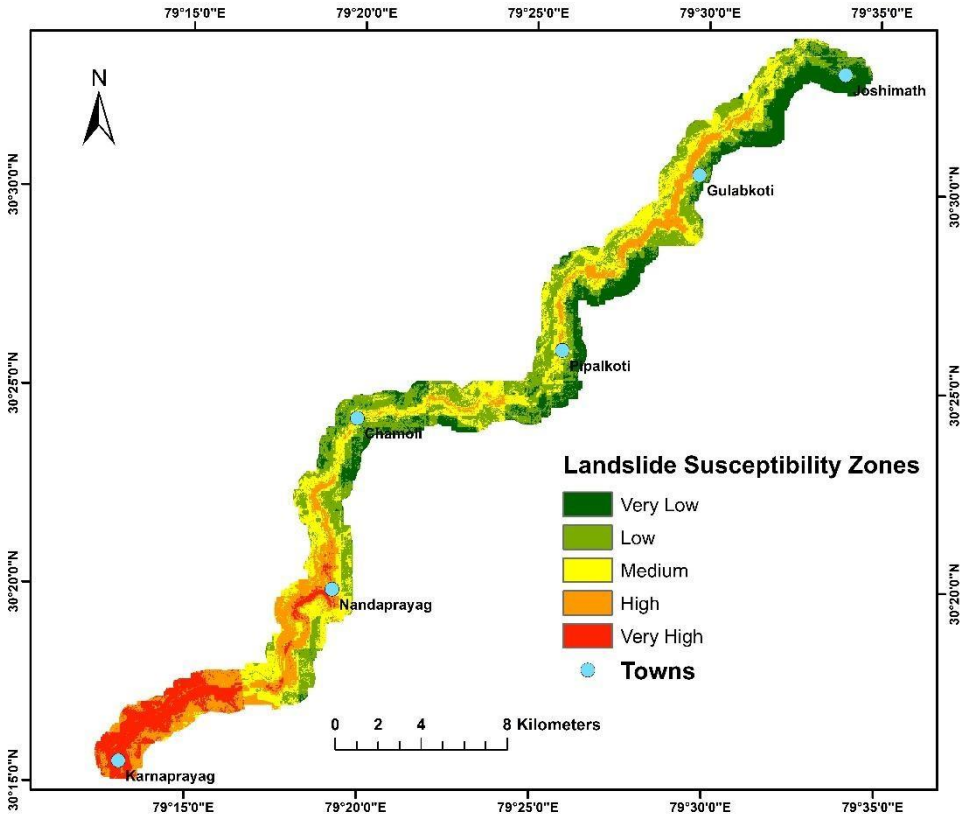

Figure 4. Landslide susceptibility map of the study area

Table 1. Spatial information of landslide conditioning elements and landslide inventory calculated by frequency ratio values

Factors	Subclass	Pixels in Domain	No of Landslides	Percent of Landslides (%)	Percent of Domain (%)	Frequency Ratio (FR)	Prediction Rate (PR)
Slope Aspect	Flat (-1)	16658	9	11.4	11.8	1.0	
	North (0-22.5)	11887	8	10.1	8.4	1.3	
	Northeast (22.5-67.5)	10212	6	7.6	7.2	1.1	
	East (67.5-112.5)	12027	11	13.9	8.5	1.7	
	Southeast (112.5-157.5)	11674	8	10.1	8.3	1.3	
	South (157.5-202.5)	11189	3	3.8	7.9	0.5	

Proceedings DOI: 10.21467/proceedings.179
ISBN: 978-81-984081-7-4

Series: AIJR Proceedings
ISSN: 2582-3922

	Southwest (202.5-247.5)	14262	7	8.9	10.1	0.9	
	West (247.5-292.5)	16633	11	13.9	11.8	1.2	
	Northwest (292.5-337.5)	18136	10	12.7	12.9	1.0	
	West (337.5-360)	18428	6	7.6	13.1	0.6	
Total						10.6	1.031
Proximity To Fault (m)	500	60257	24	30.4	41.8	0.7	
	1000	45108	32	40.5	31.3	1.3	
	1500	17220	11	13.9	11.9	1.2	
	2000	12684	8	10.1	8.8	1.2	
	>2500	8918	4	5.1	6.2	0.8	
Total						5.3	1.000
Proximity To Road (m)	200	32753	43	54.4	22.6	2.4	
	400	38042	11	13.9	26.3	0.5	
	600	39391	12	15.2	27.2	0.6	
	800	23988	11	13.9	16.6	0.9	
	1000	10451	2	2.5	7.2	0.4	
Total						4.8	3.984
Proximity To Stream (m)	400	200990	40	50.6	13.9	0.4	
	800	179078	29	36.7	12.4	0.3	
	1200	155315	10	12.7	10.8	0.1	
	1600	148064	0	0.0	10.3	0.0	
	>2000	760065	0	0.0	52.7	0.0	
Total						0.8	4.250
Elevation (m)	700-1100	35029	33	42.3	24.2	1.8	
	1100-1500	40279	15	19.2	27.8	0.7	
	1500-1900	34023	28	35.9	23.5	1.5	
	1900-2300	22395	1	1.3	15.5	0.1	
	2300-2700	13148	1	1.3	9.1	0.1	
Total						4.2	3.610
Lithology	Limestone, Dolomite and Phyllite/Slate	41089	22	27.8	28.4	1.0	
	Biotite-Tourmaline Granite and Schist/Quartzites	10958	4	5.1	7.6	0.7	
	Biotite-Garnet Schist and Gneiss	10686	3	3.8	7.4	0.5	
	Quartzites	51790	39	49.4	35.9	1.4	
	Sillimanite biotite mica Schist and Gneiss	8760	0	0.0	6.1	0.0	
	Slates/Quartzites and basic intrusives	5767	2	2.5	4.0	0.6	

Proceedings DOI: 10.21467/proceedings.179
ISBN: 978-81-984081-7-4

Series: AIJR Proceedings
ISSN: 2582-3922

	Biotite garnet Schists/Gneiss and Quartzites	15379	9	11.4	10.6	1.1	
Total						5.3	2.386
LULC	Water	4865	1	1.3	3.4	0.4	
	Trees	66830	27	34.2	46.2	0.8	
	Crops	1446	0	0.0	1.0	0.0	
	Built Area	14104	11	13.9	9.7	1.5	
	Scrub	57530	40	50.6	39.7	1.3	
Total		144775				3.9	3.398
NDVI	Water (-0.504-0.015)	7298	10	12.7	5.0	2.6	
	Builtup Area (0.015-0.14)	21906	18	22.8	15.1	1.5	
	Barren Land (0.14-0.18)	26147	17	21.5	18.1	1.2	
	Shrub and Grassland (0.18-0.27)	31158	4	5.1	21.5	0.2	
	Sparse Vegetation (0.27-0.36)	30282	12	15.2	20.9	0.7	
	Dense Vegetation (0.36-0.937)	27973	18	22.8	19.3	1.2	
Total						7.5	2.813
Plan Curvature	Concave	15218	12	15.4	10.5	1.5	
	Flat	100694	48	61.5	69.5	0.9	
	Convex	28934	18	23.1	20.0	1.2	
Total						3.5	1.501
Profile Curvature	Convex	13144	11	14.1	9.1	1.6	
	Flat	111496	56	71.8	77.0	0.9	
	Concave	20206	11	14.1	13.9	1.0	
Total						3.5	1.614
Rainfall (mm)	500-650	34364	16	20.5	23.7	0.9	
	650-800	35578	15	19.2	24.6	0.8	
	800-950	31330	5	6.4	21.6	0.3	
	950-1100	24515	8	10.3	16.9	0.6	
	1100-1250	19009	34	43.6	13.1	3.3	
Total						5.9	4.680
Seismicity	3.8-4.0	21799	6	7.6	15.1	0.5	
	4.0-4.2	26357	21	26.6	18.2	1.5	
	4.2-4.4	28499	8	10.1	19.7	0.5	
	4.4-4.6	40233	41	51.9	27.8	1.9	
	4.6-4.8	27944	3	3.8	19.3	0.2	
Total						4.6	3.340
Slope Angle (°)	<10	15751	2	2.6	11.1	0.2	

Proceedings DOI: 10.21467/proceedings.179
ISBN: 978-81-984081-7-4

Series: AIJR Proceedings
ISSN: 2582-3922

	10-20	28072	6	7.7	19.9	0.4	
	20-30	38297	27	34.6	27.1	1.3	
	30-40	32737	22	28.2	23.2	1.3	
	40-50	18651	17	21.8	13.2	1.7	
	>50	7776	4	5.1	5.5	1.0	
Total						5.9	2.267
Soil	Clay Loam	52568	44	56.4	36.3	1.6	
	Loam	92228	34	43.6	63.7	0.7	
Total						2.2	3.528
Stream Power Index (SPI)	-13.8 - -8.3	4973	1	1.3	3.5	0.4	
	-8.3 - -3.9	28892	22	28.2	20.4	1.4	
	-3.9 - 0.5	36467	14	17.9	25.8	0.7	
	0.5 - 2.3	48812	24	30.8	34.5	0.9	
	2.3 - 7.9	22140	17	21.8	15.7	1.4	
Total						4.9	1.975
Topographic Wetness Index (TWI)	5.5 - 7.5	42873	30	38.5	30.3	1.3	
	7.5 - 9.5	51935	26	33.3	36.8	0.9	
	9.5 - 11.5	26795	9	11.5	19.0	0.6	
	11.5 - 13.5	13792	10	12.8	9.8	1.4	
	13.5 - 15.5	5889	3	3.8	4.2	0.9	
Total						5.2	1.276

Table 2. Landslide susceptibility classes with existing landslide pixels

Class	Pixels in domain	No. of Landslides	Percent of Landslides (%)	Percent of domain (%)
Very Low	21821	1	1.3	16.3
Low	40064	1	1.3	29.9
Moderate	35041	8	10.3	26.1
High	24416	37	47.4	18.2
Very High	12763	31	39.7	9.5

With reference to slope aspect, slopes facing towards East has highest FR value (FR = 1.7). These slopes are most susceptible as they receive higher degree of solar radiations and precipitation, thus making them unstable [23]. According to proximity to fault map, buffer distance of 1000 m has the highest FR value (FR = 1.3) and value of FR decreases at father distances from the faults. The presence of MCT and numerous small thrusts and faults makes the region more prone to landslides [8], [24]. The highway also has a great influence on slope stability. The buffer distance of 200 m shows a higher correlation with landslides (FR = 2.4) and the value decreases as distance from the highway decreases. Landslides occur because of the displacement of resistive forces during road alignment on steep terrain due to loss of support [1], [11], [25]–[27]. In the case of elevation, the class of 700-1100 m (FR = 1.8) and 1500 – 1900 m (FR = 1.5) are highly

Proceedings DOI: 10.21467/proceedings.179
ISBN: 978-81-984081-7-4

Series: AIJR Proceedings
ISSN: 2582-3922

susceptible to landslides. The elevation range from 700-1100 m receives the highest amount of precipitation, thus making the slopes unstable. In terms of geology, the area falls in the Lesser and Higher Himalayas, showcasing the diversity of landslides with higher FR values in the Berinag/Nagthat Formation (quartzites) and Munsiari Formation (biotite garnet schist/gneiss and quartzites). In LULC, built-up areas (FR = 1.5) are most susceptible to landslides, followed by the scrub region (FR = 1.3). In the relationship of landslides and NDVI, the NDVI class of -0.504 – 0.015 has highest landslide susceptibility (FR = 2.6), followed by class of NDVI value 0.015 – 0.14. Excessive rainfall combined with steeper slopes and bare soil increases the likelihood of landslides [26], [28]. The higher FR value (FR = 1.6) of convex profile curvature depicts a higher erosion rate and higher FR value (FR = 1.5) of concave plan curvature signifies a higher probability of landslides as hollows, making the landslide debris to converge into the narrow region at the base of the slope [13]. The 1100-1250 mm rainfall class shows the strongest susceptibility to landslides (FR = 3.3). Prolonged and intense precipitation causes snow and ice to melt unusually quickly, increasing river and stream discharge and ultimately causing bank and toe erosion [2], [28]–[31]. Earthquake magnitude classes of 4.0 - 4.2 (FR = 1.5) and 4.4 - 4.6 (FR = 1.9) are highly prone to landslides. The Main Central Thrust (MCT), which represents a ductile shear zone at depth, passes through the study area near Helang [32]. This tectonic setting makes the area seismically active and thus induces landslides. The FR value increases with the increase in slope angle up to the class 40° - 50° (FR = 1.7) and then again decreases with the increase in slope angle. Shear stress in soil and stratified rock mass typically rises with increasing slope angle. According to soil type of study area, the clay loam class has a higher FR value (FR = 1.6). The increase in clay concentrations in soil mass increases the potential for landslides. FR values of classes of SPI approximately increases with the increase in the SPI value. Higher the SPI value, greater is the probability of landslides [33]. The TWI class of 11.5 -13.5 is highly susceptible to landslides (FR = 1.4).

4.1 Model validation

To validate the FR model, ROC-AUC method was chosen. The AUC model has a performance range of 0.5 to 1. AUC values of the ROC higher than 0.7 are generally considered satisfactory and values of 0.9 or higher indicate outstanding compatibility with the model [23]. The data was split into training (70%) dataset for assessing model effectiveness and testing (30%) dataset to validate the model. The success rate curve (SRC) was produced by evaluating the training data, while the evaluation of testing data generates the prediction rate curve (PRC). The AUC value of SRC for the present study is calculated to be 85.5%, while AUC value of PRC is 84.1% (Figure 5).

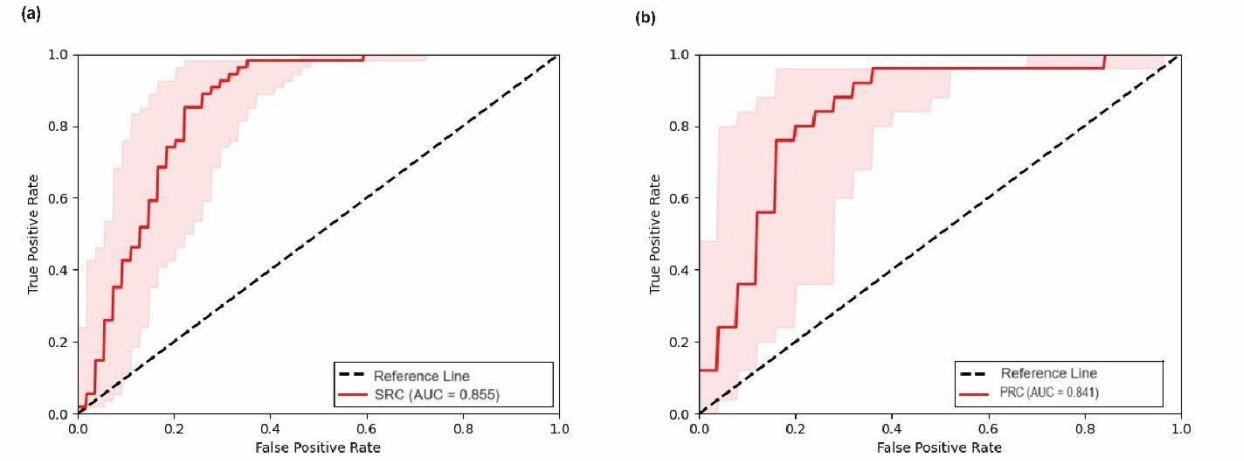

Figure 5. (a) Success rate curve (b) Prediction rate curve

Proceedings DOI: 10.21467/proceedings.179
ISBN: 978-81-984081-7-4

Series: AIJR Proceedings
ISSN: 2582-3922

5. Conclusions

The current research concentrates on the landslide susceptibility mapping along NH-7 extending from Karnaprayag to Joshimath by employing the frequency ratio method. Sixteen landslide conditioning factors were selected to assess the susceptibility of the region. The model validation was done by using ROC-AUC method. The results of the susceptibility mapping depict that rainfall is the major prompting factor for the occurrence of landslides in the study area, followed by the distance to streams and roads. Human interference for infrastructure development is making slopes unstable, causing rampant landslides in the area. The susceptibility map provides adequate knowledge of current and future landslides and is also useful for generating a risk map of the study area.

Conflict of Interest

The authors declare that they have no conflicts of interest relevant to this study.

REFERENCES

[1] V. Gupta, S. Kumar, R. Kaur, and R. S. Tandon, "Regional-scale landslide susceptibility assessment for the hilly state of Uttarakhand, NW Himalaya, India," *J. Earth Syst. Sci.*, vol. 131, no. 1, Dec. 2021, doi: 10.1007/s12040-021-01746-4.

[2] D. P. Kanungo and S. Sharma, "Rainfall thresholds for prediction of shallow landslides around Chamoli-Joshimath region, Garhwal Himalayas, India," *Landslides*, vol. 11, no. 4, pp. 629–638, Oct. 2013, doi: 10.1007/s10346-013-0438-9.

[3] S. Sarkar, D. Prasanna Kanungo, and S. Sharma, "Landslide hazard assessment in the upper Alaknanda valley of Indian Himalayas," *Geomatics, Natural Hazards and Risk*, vol. 6, no. 4, pp. 308-325, Oct. 2013, doi: 10.1080/19475705.2013.847501.

[4] J. David and T. Choki, "Landslide Susceptiblity Zoning," *Landslide Susceptibility*, pp. 113–158, 2004.

[5] F. Guzzetti, A. Carrara, M. Cardinali, and P. Reichenbach, "Landslide hazard evaluation: A review of current techniques and their application in a multi-scale study, Central Italy," *Geomorphology*, vol. 31, no. 1–4, pp. 181–216, 1999, doi: 10.1016/S0169-555X(99)00078-1.

[6] P. Reichenbach, M. Rossi, B. D. Malamud, M. Mihir, and F. Guzzetti, "A review of statistically-based landslide susceptibility models," *Earth-Science Rev.*, vol. 180, pp. 60–91, May 2018, doi: 10.1016/J.EARSCIREV.2018.03.001.

[7] S. Khanduri, "Landslide Distribution and Damages during 2013 Deluge: A Case Study of Chamoli District, Uttarakhand," *J. Geogr. Nat. Disasters*, vol. 08, no. 02, Aug. 2018, doi: 10.4172/2167-0587.1000226.

[8] B. K. Maheshwari and Sangeeta, "Earthquake-Induced Landslide Hazard Assessment of Chamoli District, Uttarakhand Using Relative Frequency Ratio Method," *Indian Geotech J*, vol. 49, no. 1, pp. 108-123, Feb. 2019, doi: 10.1007/s40098-018-0334-2.

[9] S. Sarkar, D. P. Kanungo, and G. S. Mehrotra, "Landslide Hazard Zonation : A Case Study in Garhwal Himalaya , India," *International Mountain Society*, vol. 15, no. 4, pp. 301–309, Nov. 1995, url : https://www.jstor.org/stable/3673806.

[10] T. Siddique, P. M. Haris, and S. P. Pradhan, "Unraveling the geological and meteorological interplay during the 2021 Chamoli disaster, India," *Nat. Hazards Res.*, vol. 2, no. 2, pp. 75–83, April 2022, doi: 10.1016/j.nhres.2022.04.003.

[11] P. Deshpande, P. K. Deshpande, D. C. Nainwal, and M. B. Kulkarni, "Landslide Hazard Zonation Mapping in Gopeshwar, Pipalkoti and Nandprayag Areas of Uttarakhand," *In Proceedings of the Indian Geotechnical Conference, Geotide*, Dec. 2009, pp. 16-19 https://www.researchgate.net/publication/265110255.

[12] P. K. Gautam, D. Sen Singh, D. Kumar and A. K. Singh (ed), "Landslide susceptibility modeling and slope stability mapping from Joshimath to Karnaprayag, Chamoli district, Uttarakhand, India: A Remote sensing and GIS approach," India: *Landslides Pratyush Publications*, June, 2022.

[13] D. Keshri, K. Sarkar, and S. L. Chattoraj, "Landslide susceptibility mapping in parts of Aglar watershed, Lesser Himalaya based on frequency ratio method in GIS environment," *J. Earth Syst. Sci.*, vol. 133, no. 1, Jan. 2024, doi: 10.1007/s12040-023-02204-z.

[14] USGS, "SRTM (DEM) courtesy of the US Geological Survey," usgs.gov. [Online]. Available: https://www.earthexplorer.usgs.gov [Accessed June 22, 2022].

[15] Esri., "Esri Sentinel-2 Land Cover," Esri Living Atlas. [Online]. Available: https://livingatlas.arcgis.com/landcoverexplorer/ [Accessed June 20, 2022].

[16] ESA, "Copernicus Sentinal-2," Copernicus Open Access Hub, 2022. [Online]. Available: https://browser.dataspace.copernicus.eu/ [Accessed June 26, 2022].

[17] University of East Anglia Climatic Research Unit, "CRU TS4.0: Time-series gridded climate data," British Atmospheric Data Centre (BADC). [Online]. Available: https://crudata.uea.ac.uk/cru/data/hrg/ [Accessed June 25, 2022].

[18] Bhukosh, "Landslide points data," Geological Survey of India. [Online]. Available: https://bhukosh.gsi.gov.in/ [Accessed June 10, 2022].

[19] H. G. Abdo *et al.*, "Spatial implementation of frequency ratio, statistical index and index of entropy models for landslide susceptibility mapping in Al-Balouta river basin, Tartous Governorate, Syria," *Geosci. Lett.*, vol. 9, no. 1, Dec. 2022, doi: 10.1186/s40562-022-00256-5.

[20] Binh Thai Pham, Dieu Tien Bui, Prakash Indra, and Dholakia M. B, "Landslide Susceptibility Assessment at a Part of Uttarakhand Himalaya, India using GIS – based Statistical Approach of Frequency Ratio Method," *Int. J. Eng. Res.*, vol. 4, no. 11, pp. 338–344, Nov. 2015, doi: 10.17577/ijertv4is110285.

[21] A. D. Regmi *et al.*, "Application of frequency ratio, statistical index, and weights-of-evidence models and their comparison in landslide susceptibility mapping in Central Nepal Himalaya," *Arab. J. Geosci.*, vol. 7, no. 2, pp. 725–742, 2014, doi: 10.1007/s12517-

012-0807-z.

[22] Q. Wang and W. Li, "A GIS-based comparative evaluation of analytical hierarchy process and frequency ratio models for landslide susceptibility mapping," *Phys. Geogr.*, vol. 38, no. 4, pp. 318–337, Feb. 2017, doi: 10.1080/02723646.2017.1294522.

[23] S. R. Meena, B. K. Mishra, and S. T. Piralilou, "A hybrid spatial multi-criteria evaluation method for mapping landslide susceptible areas in Kullu valley, Himalayas," *Geosci.*, vol. 9, no. 4, Apr. 2019, doi: 10.3390/geosciences9040156.

[24] I. Sarkar, A. K. Pachauri, and M. Israil, "On the damage caused by the Chamoli earthquake of 29 March, 1999," *J. Asian Earth Sci.*, vol. 19, no. 1–2, pp. 129–134, 2001, doi: 10.1016/S1367-9120(00)00021-3.

[25] S. Ghosh, M. Singh, and R. Malik, "Gis-Based Landslide Hazard Zonation Along National Highway-58, From Rishikesh To Joshimath, Uttarakhand, India," *IJARSGG.*, vol. 4, no. 2, pp. 41–55, Jan. 2016. Available: https://www.researchgate.net/publication/312023846.

[26] S. Alqadhi, H. T. Hang, J. Mallick, and A. F. S. Al Asmari, "Evaluating landslide susceptibility and landscape changes due to road expansion using optimized machine learning," *Nat. Hazards*, June 2024, doi: 10.1007/s11069-024-06652-8.

[27] P. L. Barnard, L. A. Owen, M. C. Sharma, and R. C. Finkela, "Natural and human-induced landsliding in the Garhwal Himalaya of Northern India," *Geomorphology*, vol. 40, no. 1–2, pp. 21–35, Jan. 2001, doi: 10.1016/S0169-555X(01)00035-6.

[28] J. Mey, R. Kumar Guntu, A. Plakias, I. Silva De Almeida, and W. Schwanghart, "More than one landslide per road kilometer-surveying and modelling mass movements along the Rishikesh-Joshimath (NH-7) highway, Uttarakhand, India," *NHESS*, Preprint, 2023, Available: https://doi.org/10.5194/nhess-2022-295.

[29] P. Kumar, K. Joshi, V.and Biswakarma, "Mapping of Vulnerable Landslide Zones by Large Scale Mapping in and around Devprayag Area along National Highway 58, Uttarakhand, India.," *Environ. We Int. J. Sci. Tech.*, vol. 15, pp. 145–154, Aug. 2020.

[30] M. Ramiz *et al.*, "Landslide susceptibility mapping along Rishikesh–Badrinath national highway (Uttarakhand) by applying multi-criteria decision-making (MCDM) approach," *Environ. Earth Sci.*, vol. 82, no. 24, pp. 1–22, Nov. 2023, doi: 10.1007/s12665-023-11268-5.

[31] M. Sharma *et al.*, "Assessing Landslide Susceptibility along India's National Highway 58: A Comprehensive Approach Integrating Remote Sensing, GIS, and Logistic Regression Analysis," *Conservation*, vol. 3, no. 3, pp. 444–459, Sept. 2023, doi: 10.3390/conservation3030030.

[32] K. Rajendran, C.P. Rajendran, S.K. Jain, C.V.R. Murty and J. Arleker, "The Chamoli earthquake, Garhwal Himalaya: Field observations and implications for seismic hazard," *Current Science*, vol. 78, no. 1, pp. 45-51.

[33] R. Kumar and R. Anbalagan, "Landslide susceptibility mapping using analytical hierarchy process (AHP) in Tehri reservoir rim region, Uttarakhand," *J. Geol. Soc. India*, vol. 87, no. 3, pp. 271–286, 2016, doi: 10.1007/s12594-016-0395-8.